SANDIA REPORT
SAND2022-1026
Printed January 2022

Sandia National Laboratories

Applying Waveform Correlation and Waveform Template Metadata to Aftershocks in the Middle East to Reduce Analyst Workload

Amy Sundermier
Rigobert Tibi
Christopher J. Young

Prepared by
Sandia National Laboratories
Albuquerque, New Mexico
87185 and Livermore,
California 94550

Issued by Sandia National Laboratories, operated for the United States Department of Energy by National Technology & Engineering Solutions of Sandia, LLC.

Available to DOE and DOE contractors from
U.S. Department of Energy
Office of Scientific and Technical Information
P.O. Box 62
Oak Ridge, TN 37831

Telephone: (865) 576-8401
Facsimile: (865) 576-5728
E-Mail: reports@osti.gov
Online ordering: http://www.osti.gov/scitech

Available to the public from
U.S. Department of Commerce
National Technical Information Service
5301 Shawnee Rd
Alexandria, VA 22312

Telephone: (800) 553-6847
Facsimile: (703) 605-6900
E-Mail: orders@ntis.gov
Online order: https://classic.ntis.gov/help/order-methods/

ABSTRACT

Organizations that monitor for underground nuclear explosive tests are interested in techniques that automatically characterize recurring events such as aftershocks to reduce the human analyst effort required to produce high-quality event bulletins. Waveform correlation is a technique that is effective in finding similar waveforms from repeating seismic events. In this study, we apply waveform correlation in combination with template event metadata to two aftershock sequences in the Middle East to seek corroborating detections from multiple stations in the International Monitoring System of the Preparatory Commission for the Comprehensive Nuclear-Test-Ban Treaty Organization. We use waveform templates from stations that are within regional distance of aftershock sequences to detect subsequent events, then use template event metadata to discover what stations are likely to record corroborating arrival waveforms for recurring aftershock events at the same location, and develop additional waveform templates to seek corroborating detections. We evaluate the results with the goal of determining whether applying the method to aftershock events will improve the choice of waveform correlation detections that lead to bulletin-worthy events and reduction of analyst effort.

ACKNOWLEDGEMENTS

This research was supported by the Department of State, the NNSA Office of Nuclear Verification, and the Defense Nuclear Nonproliferation R&D's Ground-based Nuclear Detonation Detection program.

We gratefully acknowledge the contributions of Andrea Conley, Ellen Syracuse, and Tim Evans, who reviewed drafts of the report.

CONTENTS

LIST OF FIGURES

LIST OF TABLES

This page left blank

ACRONYMS AND DEFINITIONS

Abbreviation	Definition
ARID	Arrival Identifier
CSS	Center for Seismic Studies
CTBT	Comprehensive Nuclear-Test-Ban Treaty
CTBTO PrepCom	Preparatory Commission for the Comprehensive Nuclear-Test-Ban Treaty Organization
FAR	False Alarm Rate
IDC	International Data Centre
IMS	International Monitoring System
LEB	Late Event Bulletin
LTA	Long-Term Average
NDEF	Number of Defining Phases. In the CSS standard, NDEF is defined as the number of locating phases.
ORID	Origin Identifier
PTS	Provisional Technical Secretariat of the CTBTO PrepCom
REB	Reviewed Event Bulletin
SNR	Signal-to-Noise Ratio
SNL	Sandia National Laboratories
STA	Short-Term Average
STA/LTA	Ratio of Short-Term Average over Long-Term Average

1. INTRODUCTION

Recurring events such as earthquake aftershocks and mining blasts increase the number of seismic events that are detected on global networks such as the International Monitoring System (IMS) and thereby increase analyst workload to produce a bulletin. For that reason, monitoring organizations have shown interest in adopting techniques such as waveform correlation to quickly characterize recurring events to reduce the amount of effort required by analysts to produce a high-quality event bulletin. During 2019 and 2020, members of the Provisional Technical Secretariat (PTS) of the Preparatory Commission for the Comprehensive Nuclear-Test-Ban Treaty Organization (CTBTO PrepCom) invited several experts familiar with waveform correlation methods to participate in a study of recurring events that are particularly problematic for the International Data Centre (IDC). The goal of that research study was to reduce analyst workload in monitoring system pipelines due to aftershocks [1] and mining blasts [2][3].

A subsequent study of mining blasts [4] expanded upon the waveform correlation detections by adding steps after the initial correlation detection. These include using metadata information associated with the template event (i.e. the set of detecting stations and the phases they detected) to develop a set of hypothesized arrivals that can provide corroborating evidence for the detection. The purpose of the additional processing steps is to select the waveform correlation detections that are most likely to result in bulletin-worthy events and simultaneously gather the evidence of corroborating arrivals that are consistent with the detection of repeating events, thus reducing workload on the analysts. This study applies a similar method to aftershock events that uses template event metadata to select detections that are likely to lead to corroborating evidence for the detection. Aftershocks that follow large magnitude events constitute an operationally challenging environment for a global seismic monitoring system such as the IDC because the high event rate makes it more difficult for the automated pipeline to correctly associate seismic arrivals to the events. During a large aftershock sequence, the increased workload required to produce the analyst-reviewed bulletins may delay the publication of the bulletins.

The authors used SeisCorr, a software system developed at Sandia National Laboratories (SNL) for waveform correlation event detection that has been used for studies of aftershock sequences [1][5][6], and general regional seismicity, including mining regions [2][3][4]. In this study of two aftershock sequences in the Middle East region, we use template event metadata to create waveform templates for the set of stations that would be likely to detect a repeating event. We apply waveform correlation using the set of potentially corroborating templates to determine if there is evidence of a repeating event shown by the consistency of relative detection times. We present examples of repeating events that were detected using the method. We review the results to evaluate whether the method shows promise for reducing analyst workload by selecting the most useful detections to bring to the attention of seismic analysts in the presence of aftershock sequences during global monitoring.

2. EXPERIMENTAL METHODS

Aftershocks are well-suited to detection by waveform correlation because the events with similar mechanisms are repeated over a small geographic area and the same set of stations will be likely to record the signals. However, aftershocks may occur so frequently that the recorded waveforms overlap in time, confounding the matched filter hypothesis of waveform correlation that assumes only one signal is present within a windowed time period. Moreover, overlapping waveforms may occur in templates as well as detection windows, further complicating the process of curating a useful template library.

Our method explores empirical results from a search for corroborating arrivals based on template event metadata for two aftershock sequences in the region of the Middle East. Table 2-1 shows information about the main shocks, the geographical and temporal extents of the templates, and the one week post main shock time intervals of continuous waveforms that were actually processed to detect aftershocks. The geographical extents for our templates for both the 2017 Iran/Iraq border earthquake and the 2020 Crete earthquake are given as a 2-degree radius around the epicenter of the main shock. For both aftershock sequences our template libraries were created from aftershock events in the first 24 hours after the main shock, but we also included templates from events for a period prior to the main shock to investigate the potential effectiveness of using foreshocks within the same 2-degree radius of the main shock. The amount of time used to find foreshocks for each mainshock was chosen to ensure a sufficient number of foreshocks were found (one month for the Iran/Iraq event, 3 months for the Crete event).

Table 2-1. Aftershock geographical and temporal extents.

Aftershock Sequence	Main Shock Origin Time (UTC)	Geographical Extent (Lat, Lon)	Temporal Span of Templates (UTC)	Temporal Span of Detections (UTC)
2017 Iran/Iraq Border	11/12/2017 18:18	Within 2.0 degrees of (34.905N, 45.956E)	10/12/2017 00:00 -- 11/13/2017 18:18	11/13/2017 18:18 -- 11/20/2017 18:18
2020 Crete	05/02/2020 12:51	Within 2.0 degrees of (34.182N, 25.710E)	02/01/2020 00:00 – 05/03/2020 12:51	05/03/2020 12:51 – 05/10/2020 12:51

Table 2-2 shows the stations that were chosen for each aftershock sequence to make template waveforms. We preferred stations within the Middle East region because waveform correlation performs best with templates of a high time-bandwidth product at local to regional distances. IMS primary seismic stations and arrays are preferred (IMS Treaty Codes PS**), but auxiliary seismic stations (IMS Treaty Codes AS***) that were near the mainshock epicenters and detected many aftershock events were also included in station processing. For example, in the case of the 2020 Crete earthquake, the IMS station nearest to the earthquake was auxiliary seismic station IDI (AS036) in Anogia, Greece. Because IDI is closer to the event than any of the primary stations, the IDI templates have a high signal-to-noise (SNR) ratio.

Table 2-2. Stations chosen for each aftershock sequence.

Aftershock Sequence	Station Name	Array Code	IMS Treaty Code	Number of Channels Processed
2017 Iran/Iraq Border	Tel Al Asfar, Jordan	ASF	AS056	3
	Keskin Array, Turkey	BRTR	PS43	6
	Alibeck Array, Turkmenistan	GEYT	PS44	7
	Khabaz, Russia	KBZ	PS32	3
	Mount Meron Array, Israel	MMAI	AS049	14
	Wadi Sarin, Oman	WSAR	AS074	3
2020 Crete	Tel Al Asfar, Jordan	ASF	AS056	2
	Keskin Array, Turkey	BRTR	PS43	6
	Anogia, Greece	IDI	AS036	3
	Mount Meron Array, Israel	MMAI	AS049	14

The focus of this research project is to explore using template event metadata to find stations that are most likely to provide corroborating detections after an initial waveform correlation detection; this improves the credibility and usefulness of the initial detection. Monitoring organizations using sparse networks have been slow to adopt traditional waveform correlation because the method can produce many additional events for analysts to review, both real and false, hence actually increasing analyst workload. This study seeks to bridge the gap between all waveform correlation detections and waveform correlation detections that reduce workload on the analysts, which we term bulletin-worthy events. The correct selection of waveform correlation detections can reduce the workload of analysts when the detections are seen at the same group of stations for a repeating event.

In the case of aftershocks, we anticipate that aftershocks of a similar magnitude should be detected by the same group of stations. To explore this hypothesis, we chose some example waveform correlation templates that detect aftershocks repeatedly at a station near the location of the main shock. We examine template event metadata to discover the group of stations that detected the template event and are therefore likely to detect the same aftershocks. Template libraries are created

for that group of stations and are then correlated against continuous waveform data in order to validate the detections at the original station. We present examples of the results from this approach and discuss the benefits and disadvantages for the two aftershock sequences studied.

The study was conducted using the SeisCorr software for waveform correlation [4][5][4][6][7]. SeisCorr supports three major activities for waveform correlation research: 1) template preparation; 2) correlation of template waveforms with continuous waveform data to detect possible events; and 3) candidate event creation from multistation validation.

For this study the basic SeisCorr detections were followed by steps that use template event metadata to discover other stations that are likely to corroborate the detection. The following is an overview of the approach [4]:

- Waveform cross correlation uses template waveforms from historical seismic events to detect recurring events from the same seismic source.
- Effective waveform cross correlation requires templates with broad frequency content to produce reliable single-station detections over a broad area, but because high-frequency signals attenuate strongly over distance, such high-quality templates with broad frequency content only exist for stations at local to near-regional distances from the target seismic sources.
- Our research seeks to improve the effectiveness of waveform cross correlation detections for sparse global networks through use of template event metadata and network analysis of corroborating stations.
- A network-focused perspective of recurring events improves the credibility of detections, since the number of stations that detected the template event originally, in combination with the relative amplitude of recurring detection, enables estimation of how many stations are likely to detect the subsequent event. Thus, we select bulletin-worthy waveform correlation detections to reduce analyst workload.

SeisCorr contains functionality for the creation of a template library for a given station based on a query of the database arrival table. Seismic arrivals were sought for LEB events located within two degrees of the epicenter of the main shock during the first 24 hours of the aftershock sequence. We chose to use the Pn, Sn, and Lg phases from LEB arrivals depending upon the station's distance from the main shock; the SeisCorr user queries for labeled arrivals of the desired phases at the chosen station. SeisCorr allows the user to filter the waveforms associated with each arrival using a bandpass filter chosen to work well for the epicentral distance of the recording station. The SeisCorr user may screen the filtered waveforms based on a specified short-term average/long-term average (STA/LTA) threshold to eliminate waveforms with low SNR, resulting in a set of candidate templates. The candidate templates can be saved as a template library for the station.

We use the term "candidate template" to recognize that even after the SNR-screening step, not all arrival waveforms will make acceptable templates for correlation. Additional screening steps may be applied to eliminate poor quality templates. For example, templates that contain a high amplitude spike may correlate with non-colocated signals and noise with a correlation coefficient that exceeds the correlation threshold. This issue can result in thousands of false detections from a single template with a spike characteristic in the waveform. We review the correlation results and remove defective templates, then run the correlations again until the template library is free of templates that match thousands of unwanted waveforms. This does not eliminate all false detections, but it

removes the most egregiously false detectors from the template library. In the case of an aftershock sequence, a waveform template may legitimately match hundreds of aftershock waveforms, so reviewing aftershock templates that result in many detections was an interactive task for this research study.

Prior waveform correlation research at SNL demonstrated the importance of choosing a correlation coefficient threshold that is dependent on the characteristics of the template [7]. In theory, the distribution of correlation values obtained from correlating a template with a continuous data stream can be thought of as the sum of two distributions: 1) correlation of the template with noise and 2) correlation with similar events. SeisCorr implements a sophisticated algorithm for setting template thresholds based upon a false alarm rate (FAR) obtained from correlation with noise for each correlation threshold. Ordinarily, unless similar events can be identified and cut out first, correlating a template with continuous data will generate both noise and signal correlations. However, time-reversing the template ensures the template has the same time-bandwidth product as the template proper and should yield a very similar distribution of correlation values with noise windows while also not correlating with similar events, even if they are present. Thus, a time-reversed template can be correlated with continuous data to generate a robust distribution of noise correlation values, even without first screening out time windows with similar events. Using this method, thresholds can be set individually for each template to achieve a consistent FAR based on noise correlations.

Prior studies [8][9][10] have shown that for a template waveform with a low time-bandwidth product (e.g., teleseismic P) a threshold based solely on the noise distribution may be too low because correlation with signals from some non-similar events do not fit within the noise distribution, nor are they part of the target signal distribution. For this study of aftershock sequences, we created templates from stations at regional distances and choose long time windows ranging from 60s to 260s; thus, we expect a time-bandwidth product high enough to separate the signal characteristics from noise. The template thresholds were set by the time-reverse method implemented in SeisCorr such that the noise correlation thresholds were set by processing continuous waveforms during the aftershock sequence, i.e., we intentionally chose a time period with many similar events in it. Thus, the thresholds set for this study were based not only on correlation with noise but also with the signals of the numerous aftershock events in the continuous data. More research is needed to develop an optimal approach to setting thresholds for template waveforms for aftershocks since the approach used in this study must be modified for an operational system. Our approach violated the antecedent constraint by using waveform data from the study period to set template thresholds to detect events.

There are several steps required to create a template library in SeisCorr using an event bulletin as a source for template events:

1. Choose relevant event origins from an existing bulletin (e.g., LEB ORIGIN table from the IDC). This step creates a set of origin candidates for templates and for convenience these origins may be stored in an ORIGIN table based on the Center for Seismic Studies (CSS) schema that is specific to the region and study period.
2. Create a table from a query of candidate template associations for the origins found in step 1 (i.e., an ASSOC table from the CSS schema).
3. Create a table from a query of candidate template arrivals for the origins and associations found in steps 1 and 2 (i.e., an ARRIVAL table from the CSS schema).

4. Choose stations for which we want template libraries by reviewing the number of seismic arrivals at each station that detected the events from step 1, the number of regional seismic phases that were detected, and the SNR of the detected waveforms. For each station, steps 5 through 10 create a template library for that station.
5. Use SeisCorr to query for arrivals at a station. The query uses the candidate template events and candidate template associations from steps 1-3 along with a specified phase list and a time window containing the arrival time.
6. Select a template window size and offset from the picked arrival time. The template window size is the same time duration for the entire library in the current version of the SeisCorr software.
7. Choose a filter band based on the epicentral distance and filter the templates to enhance the signal. The filter band is the same for the entire library in the current version of the software.
8. Run an STA/LTA detector on all the templates in the library. Select an STA/LTA threshold and discard candidate templates that do not meet the threshold. This step is optional if all the templates appear to have a good SNR.
9. Save candidate templates for the station as a library. For arrays, the templates include a waveform for every array element. For three-component stations, the template contains three waveforms representing the north, east, and vertical components.
10. Set correlation coefficient threshold using the time-reverse method.

The 2017 Iran/Iraq Border aftershock sequence was challenging for a waveform correlation study because there were only 39 candidate template events within the first 24 hours after the main shock based on arrivals from regional phases Pn, Sn, and Lg. Few of the stations yielded templates that passed the STA/LTA threshold test and the background was noisy, which is typical during an aftershock sequence. In contrast, the 2020 Crete aftershock sequence had 135 candidate template events within the first 24 hours after the main shock based on arrivals from regional phases Pn, Sn, and Lg and the stations yielded more templates that passed the STA/LTA threshold test.

Step 4 from the list above chooses the stations for which template libraries are created. Table 2-3 shows the number of events detected by regional seismic phases Pn, Sn, and Lg for the first 24 hours of the two aftershock sequences, listed by detecting station. The events are limited by the geographic and temporal extents of Table 2-1. The events in this table provide the total pool of candidate template events for waveform correlation templates. Only a subset of the stations listed in the table were included in this study; in some cases, data were not available in our waveform archive or exhibited poor quality during the aftershock study period.

Table 2-3. The number of events detected by regional seismic phases Pn, Sn, or Lg for the first 24 hours of the aftershock sequences, listed by detecting station in alphabetical order.

2017 Iran/Iraq Border Aftershocks	
Station	Number of Events
ASF (Jordan)	29
BRTR (Turkey)	21
EIL (Israel)	22
GEYT (Turkmenistan)	21
GNI (Armenia)	26
IDI (Greece)	4
KBZ (Russia)	17
KVAR (Russia)	8
MMAI (Israel)	28
WSAR (Oman)	32

2020 Crete Aftershocks	
Station	Number of Events
AKASG (Ukraine)	98
ASF (Jordan)	58
BRTR (Turkey)	108
DAVOX (Switzerland)	10
EIL (Israel)	98
GERES (Germany)	32
GNI (Armenia)	24
IDI (Greece)	109
KBZ (Russia)	65
KEST (Tunisia)	36
KVAR (Russia)	26
MLR (Romania)	36
MMAI (Israel)	104
VAE (Italy)	42
VRAC (Czech Republic)	35

Steps 5-10 create template libraries determined by a set of parameters that are applied to the template waveforms, such as template window length, filter bands, and thresholds that may be applied to the templates. For example, during step 8 template waveforms with a low SNR may be removed through the use of a STA/LTA that compares the amplitude of a portion of the template to the amplitude of the preceding noise

Table 2-4 provides an overview of the template library parameters for the aftershock sequences, organized by station. The phase arrivals were reviewed for each station to determine what phase would make the best template library for the station. We preferred to make templates from the Pn phase pick and include most of the waveform. However, for stations MMAI and WSAR, we found that the LEB bulletin had Lg and Sn picks, respectively, that provided good quality templates; hence, these stations have two template libraries, based on Pn and Lg/Sn for the 2017 Iran/Iraq Border aftershock sequence. The number of templates in the template library for each station is indicated by the Template Count column.

Table 2-4. Template Library Parameters for Aftershock Sequences

	Stations	Phase	Window Length (s)	Filter Band (Hz)	STA/LTA parameters (s)	STA/LTA Threshold	Template Count
2017 Iran/Iraq Border	ASF	Pn	260	0.8-12.0	N/A	N/A	26
	BRTR	Pn	60	0.8-3.5	1/30/0	2.5	10
	GEYT	Pn	60	0.8-3.5	1/30/0	2.5	8
	KBZ	Pn	60	0.8-3.5	3/30/0	2.5	15
	MMAI	Pn	60	0.8-3.5	3/30/0	2.5	3
	MMAI	Lg	60	0.8-3.5	30/60/200	2.0	10
	WSAR	Pn	60	0.8-3.5	3/30/0	2.5	26
	WSAR	Sn	80	0.8-3.5	N/A	N/A	17
2020 Crete	ASF	Pn	200	1.0-6.0	3/30/0	3.0	33
	BRTR	Pn	80	0.8-6.0	1/30/0	3.0	42
	IDI	Pn	80	1.0-12.0	N/A	N/A	133
	MMAI	Pn	140	0.8-8.0	3/30/0	2.0	54

* Station STA/LTA parameters represent "short-term average window / long-term average window / gap between windows" (e.g., "1/30/0"). Note that for the MMAI Lg templates, the gap between STA and LTA is large (200s) such that the LTA is computed prior to the Lg's corresponding P arrival.

Figure 2-1 shows a template (red waveform) from an aftershock during the first 24 hours of the 2020 Crete aftershock sequence that was detected by station IDI on May 2, 2020. That template

later detected 36 aftershocks with a correlation score above the correlation threshold; only the 10 detected waveforms (blue) with the highest correlation scores are shown in the figure. That template shows the potential benefit of applying waveform correlation to aftershock sequences to find additional events because only one of the ten blue waveforms shown was included in the IDC LEB. This waveform is shown second from the top with a labeled Pn pick and detection time of May 4, 2020 at 04:14:08. The first blue waveform from the top had a detection time of May 7, 2020 at 10:16:02 UTC and a correlation score of 0.9547, which indicates a very high similarity with the red template waveform; yet it was not picked as an aftershock for the bulletin. The separate event waveform that precedes the detection window delineated by vertical red lines may have prevented proper association of the aftershock waveform between the red lines because the automated processing was unable to recognize the independent sources of the waveforms. Overlapping waveforms are a very common problem during aftershock sequences due to the high event rate, resulting in a challenging operating environment for global seismic monitoring organizations. Figure 2-2 shows an example of a series of overlapping event waveforms detected by station IDI within an hour of the 2020 Crete main shock, illustrating the difficulty in isolating template waveforms during the first 24 hours of the aftershocks from a major quake. This figure also shows the wide variation in magnitude for aftershocks during a 10-minute time period, which can be observed by comparing the amplitude of the signal to the noise level.

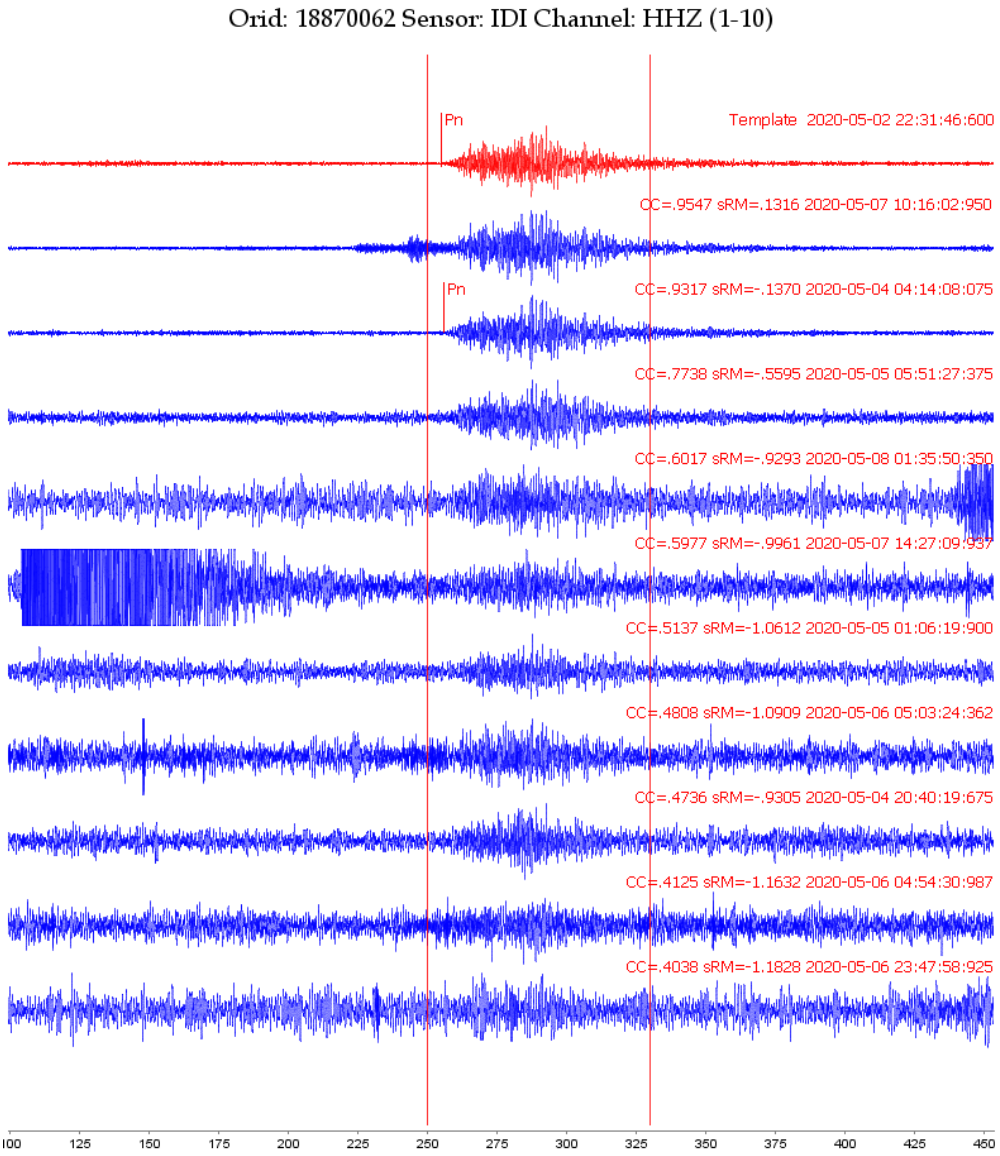

Figure 2-1. Waveform template (red) and detections (blue) for a Pn template from station IDI for event origin 18870062. The long red vertical lines indicate the window of the 80 s template, which begins 5 s before the picked Pn arrival. The short red vertical lines labeled Pn represent picked Pn phase arrivals from the LEB. The figure shows only the vertical component, HHZ, but the template also includes waveforms from the HHE and HHN components.

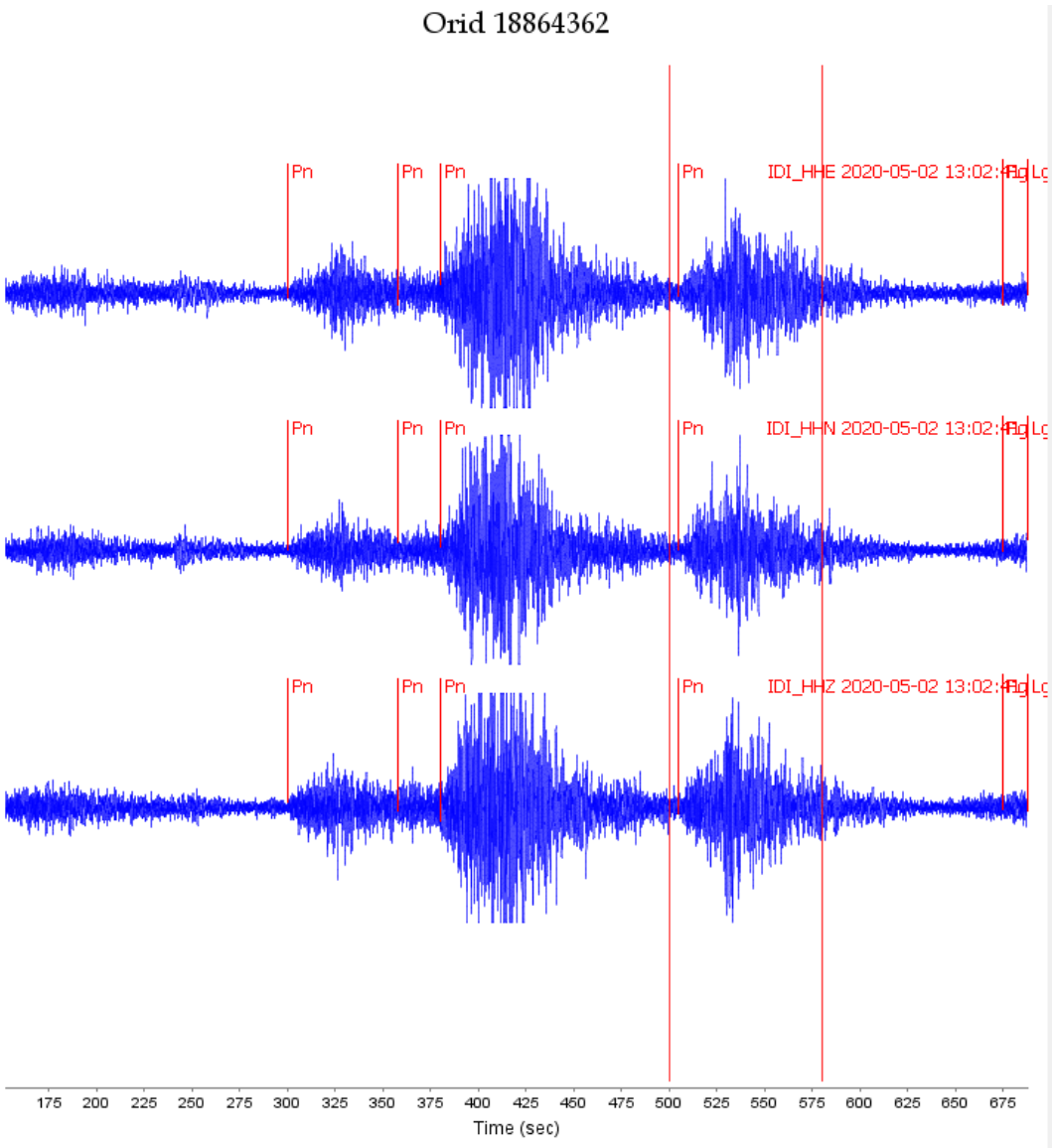

Figure 2-2. Three-component waveforms (HHE, HHN, HHZ) for a series of Pn arrivals detected at station IDI. The red vertical lines indicate the window of an 80 s template based on event origin 18864362, which begins 5 s before the Pn arrival detected on May 2, 2020 at 13:02 UTC.

This study applies an extension to traditional waveform correlation by using template event metadata to find additional stations that were likely to detect the same events. This method to detect corroborating arrivals at other stations was shown to be successful for improving detections of mining blast events in Wyoming and Scandinavia [4]. This study evaluates whether the same method will work well for aftershock sequences. The example waveform correlation template and detections by array BRTR (Figure 2-3) serve as the starting point for presentation of the method by representing an initial traditional waveform correlation detection by a single template.

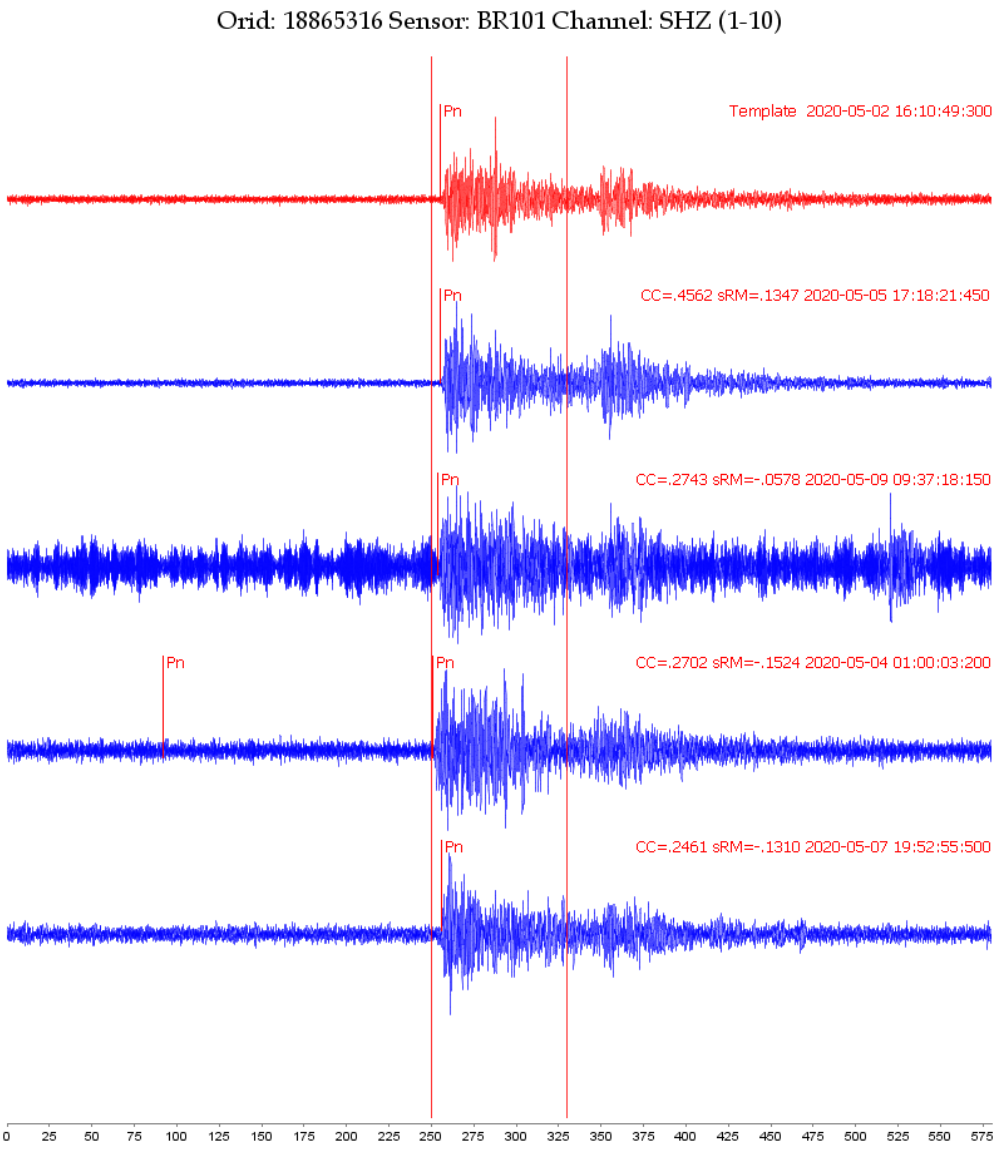

Figure 2-3. Waveform template (red) and detections (blue) for a Pn template for station BRTR. The red vertical lines indicate the window of the 80 s template based on event origin (ORID) 18865316, which begins 5 s before the Pn arrival detected on May 2, 2020 at 16:10:49 UTC. The figure shows only one array element, BR101, but the template includes waveforms from all 6 SHZ elements of the BRTR array. The four aftershocks detected by the template were included in the LEB, as indicated by the Pn pick (short vertical red bar labeled Pn).

After the initial correlation detection shown in Figure 2-3, the metadata from the template event ORID 18865316 is used to compile the list of expected arrivals from a potential repeating aftershock event that would be recorded at other stations of the network. The list of associated arrivals from the template event (Table 2-5) provides the group of potential corroborating template waveforms. For this study, we used regional Pn, Sn, and Lg arrivals to ensure a high time-bandwidth template. Templates that include multiple phases can be especially effective because the distance of the repeating event from the station is constrained by the differential arrival time between the phases, thus improving the credibility of the detection. However, during an aftershock sequence very long

template windows are more likely to have overlapping signals in the template waveform and/or the continuous waveforms that are correlated with the template, reducing the likelihood of a correlation match.

Table 2-5. Template event origin 18865316 LEB metadata for associated arrivals showing detecting station, associated seismic phase, and arrival time.

STA	PHASE	Arrival Time (UTC)
IDI	Pn	02-MAY-20 16.13.25
MMAI	Pn	02-MAY-20 16.14.58
BRTR	Pn	02-MAY-20 16.15.04
EIL	Pn	02-MAY-20 16.15.10
ASF	Pn	02-MAY-20 16.15.17
VAE	Pn	02-MAY-20 16.15.18
MLR	Pn	02-MAY-20 16.15.43
KEST	Pn	02-MAY-20 16.16.11
GNI	Pn	02-MAY-20 16.16.52
VRAC	Pn	02-MAY-20 16.16.53
KBZ	Pn	02-MAY-20 16.16.54
KVAR	Pn	02-MAY-20 16.16.54
AKASG	Pn	02-MAY-20 16.16.55

Associated arrivals for the template event 18865316 identify stations that are most likely to detect the same repeating aftershock events. Template libraries are created for that group of stations to corroborate detections by other stations in the group. For this example, templates were made for two three-component stations, IDI and ASF, and for one additional array, MMAI. Other parameters used for template library preparation are shown in Table 2-4.

Waveform correlation performs well with a high time-bandwidth product; thus, a broad frequency band filter is preferred to retain individual characteristics of the signal at the expense of a template that exhibits more background noise. It may be possible to apply denoising techniques [11] to improve the SNR of the signal while retaining an even higher time-bandwidth template, but this remains for future work. For the 2020 Crete aftershock template libraries, a broad range of frequencies likely to produce a credible correlation match was prioritized higher than maximizing the SNR of the signal.

The time-reverse method [7] sets cross-correlation thresholds for templates with a desired false alarm rate (FAR) of 1 FA/year; the threshold is calculated for each template resulting in a customized threshold value. The reversed templates were correlated against the week-long temporal

period of desired aftershock detections (Table 2-1) to set a threshold value that excludes background noise detections during a period of heightened noise levels due to the high event rate.

SeisCorr correlates template waveforms with continuous waveform data for each station to seek evidence for repeating event hypotheses. The correlation detections for templates based on LEB ORID 18865316 from stations IDI, MMAI, BRTR and ASF are shown in Figure 2-4.

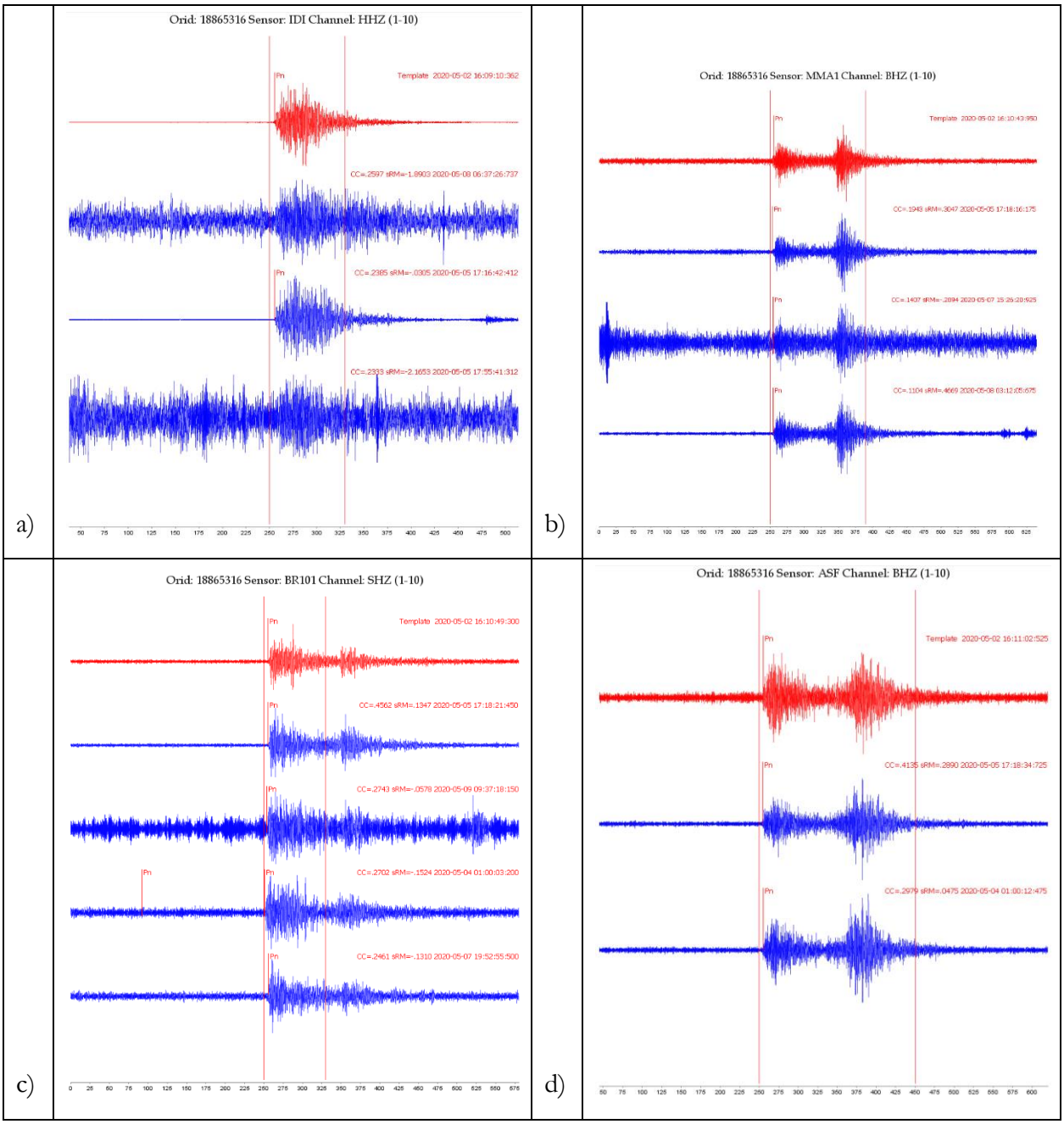

Figure 2-4. Templates (red) based on LEB ORID 18865316 and corresponding correlation detections (blue) to show corroborating detections for repeating events. Template windows are indicated by vertical red lines. For three-component stations IDI and ASF, only the vertical component is shown. For arrays MMAI and BRTR, only the vertical component of the first array

element is shown. a) Pn at IDI. b) Pn at MMAI, where the template includes multiple seismic phases. c) Pn at BRTR. d) Pn at ASF, where the template includes multiple seismic phases.

We calculate time differences relative to the initial template times and initial detection times to look for consistency in seismic arrival time that would be expected for the repeating event detected on May 5, 2020 at array BRTR with arrival time 17:18:21 (Table 2-6); coherent detections by all four stations provide convincing evidence. Effectively, we are checking to see that the origin time for the detected event at each station is in agreement, indicating that all stations are detecting the same event. For simplicity, the template time and detection time are used for this calculation; the template starts 5 s prior to the picked arrival in all templates, so the template time precedes the arrival time. The last two columns in the table show the times relative to BRTR with agreement for all relative times. Small discrepancies are likely due to a slight difference between the location of the template event and the location of the detected event. This approach has a further advantage in that a location for the detected repeated event can be calculated if there are enough corroborating detections.

Table 2-6. Table of relative time calculations for corroborating templates from LEB ORID 18865316 and detections from correlation, ordered by arrival time.

LEB ORID 18865316					
Station	Phase	Template date/time (UTC)	Detection date/time (UTC)	Difference in Template Times Relative to BRTR (s)	Difference in Detection Times Relative to BRTR (s)
IDI	Pn	5/2/20 16:09:10	5/5/20 17:16:42	-99	-99
MMAI	Pn	5/2/20 16:10:43	5/5/20 17:18:16	-6	-5
BRTR	Pn	5/2/20 16:10:49	5/5/20 17:18:21	0	0
ASF	Pn	5/2/20 16:11:02	5/5/20 17:18:35	13	14

3. RESULTS

This empirical study explores application of a method to aftershocks that was demonstrated to detect repeating mining blasts in a prior study [4]. That study used template event metadata to find stations that could possibly corroborate an initial waveform correlation detection and applied the method to two mining regions as a proof-of-concept study. This study is also a proof-of-concept, and we chose the 2020 Crete aftershock sequence and the 2017 Iran/Iraq border aftershock sequence for the evaluation.

3.1. 2020 Crete Aftershocks

The example event in Table 2-6 was detected by templates based on LEB ORID 18865316 and shows that the method explored by this study has promise. However, Figure 2-4 shows additional detections by the same templates that are not corroborated by the other stations. For example, BRTR (Figure 2-4 c) and ASF (Figure 2-4 d) both detect arrivals on May 4, 2020 at 01:00 UTC. This result suggests that stations IDI and MMAI should also have detected that event with templates based on LEB ORID 18865316, but they did not. Moreover, there were single station detections by the same templates that were not detected by any of the other three stations. There is a lack of consistency in template detections based on the same template event when applying the method to aftershock events; the method showed greater consistency when applied to mining blasts. The examples in this section illustrate some of the issues that were discovered and form the basis for results and conclusions.

Template libraries for the 2020 Crete aftershock sequence were created for four stations: IDI, MMAI, BRTR, and ASF. These stations detected large numbers of aftershock events within the first 24 hours of the aftershock sequence (Table 2-3) and were found to detect the same events when the LEB events were analyzed; thus, we expect that templates based on the same LEB ORID would be likely to detect repeating events. Yet this was not found to be as common as expected. For example, the IDI template based on LEB ORID 18870062, shown in Figure 2-1, has many detections. However, none of the other three stations, MMAI, BRTR, or ASF, detected the same events with templates based on LEB ORID 18870062. In the case of BRTR, there was no template in the station library, because the waveforms had low SNR waveforms and failed to meet the STA/LTA threshold test. The template for array MMAI contains a high frequency anomaly on a subset of the channels that begins near the end of the template window and persists for several hundred seconds (Figure 3-1 a). This anomaly does not appear to be due to a real seismic event; nevertheless it caused false detections during library testing by correlating above the detection threshold with similar anomalies at other times (Figure 3-1 b). In the case of ASF, there was a template, but it detected no events.

Other stations listed in Table 2-3 that detected large numbers of 2020 Crete aftershocks during the first 24 hours were evaluated for development of template libraries but were discarded. AKASG (Figure 3-1 c, d) and KBZ (Figure 3-1 e, f) exhibited data recording problems during the first 24 hours of the aftershock sequence and were not used for templates. Our data archive did not have waveforms for auxiliary station EIL during the first 24 hours of the aftershock sequence, so this station was not processed.

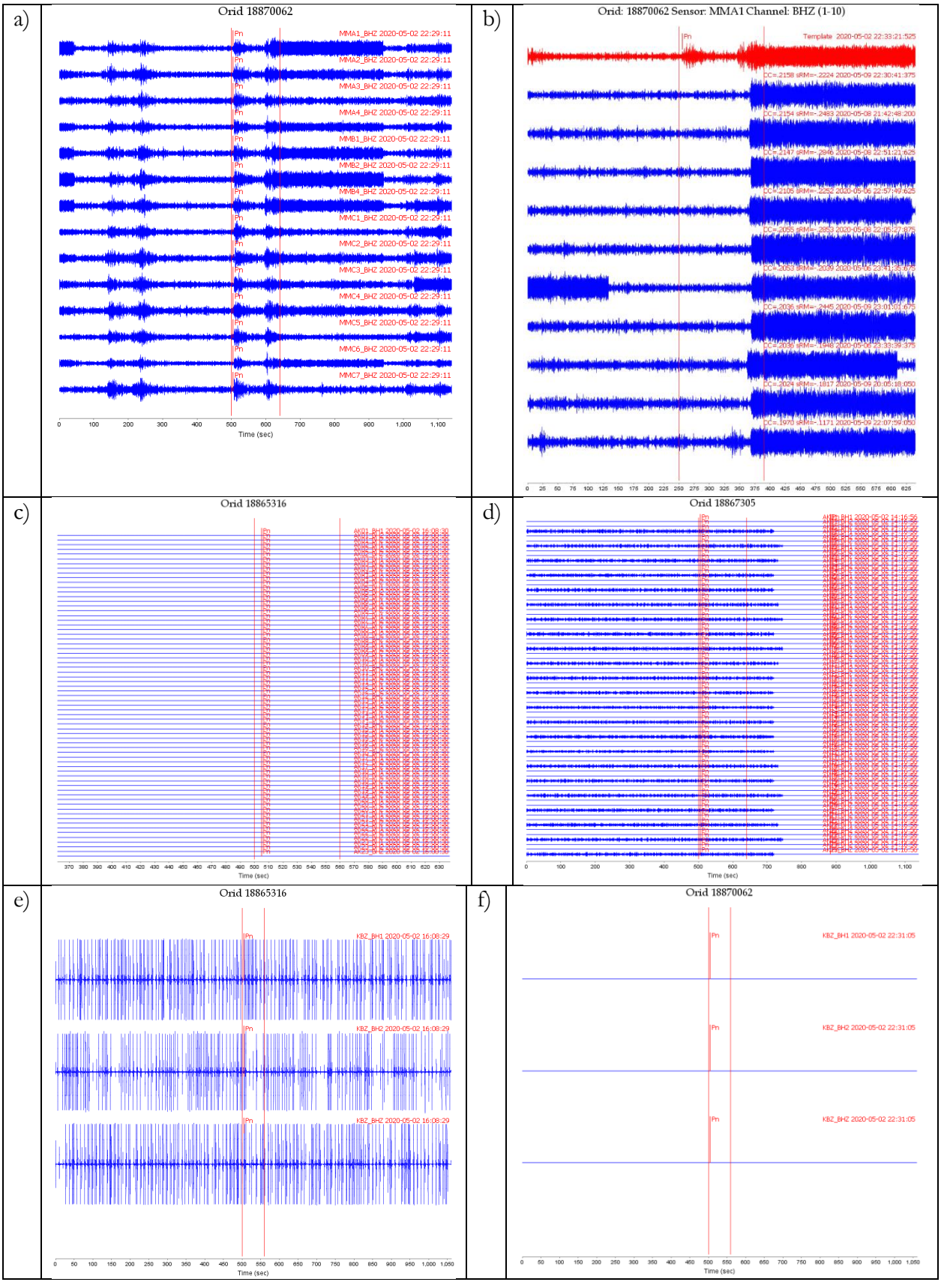
a)
Orid 18870062
Time (sec)
b)
Orid: 18870062 Sensor: MMA1 Channel: BHZ (1-10)
c)
Orid 18865316
Time (sec)
d)
Orid 18867305
Time (sec)
e)
Orid 18865316
Time (sec)
f)
Orid 18870062
Time (sec)

Figure 3-1. Templates (red) and correlation detections (blue) exhibiting data recording problems during the first 24 hours of the 2020 Crete aftershock sequence. a) MMAI template based on LEB ORID 18870062 shows a high frequency anomaly near the end of the template window. All array channels are shown for the template. b) False correlation detections by the MMAI template due to the presence of a high frequency anomaly at the end of the template window. Only the vertical BHZ channel of MMA1 array element is shown. c) Data recording failure at array AKASG for Pn arrival associated with template ORID 18865316. The template includes all array channels. d) Data recorded at array AKASG for Pn arrival associated with template ORID 18867305. The template window shows waveform data, but there is a data failure during the latter part of the period shown. e) Data recorded at three-component station KBZ for Pn arrival associated with template ORID 18865316, showing a problem with the recorded waveform. f) Data recording failure at three-component station KBZ for Pn arrival associated with template ORID 18870062.

Figure 3-2 shows an example set of templates based on LEB ORID 18869813 for stations IDI and BRTR and resultant correlation detections. MMAI and ASF had no templates based on this LEB event. Station IDI was nearest to the event and had 27 waveform correlation detections (only the first 10 detections are shown in the figure). In contrast, array BRTR had only three waveform correlation detections, all of which correspond to LEB bulletin events and thus are legitimate events. Station IDI corroborated two of the three BRTR detections, which is shown by the calculation of relative times in Table 3-1.

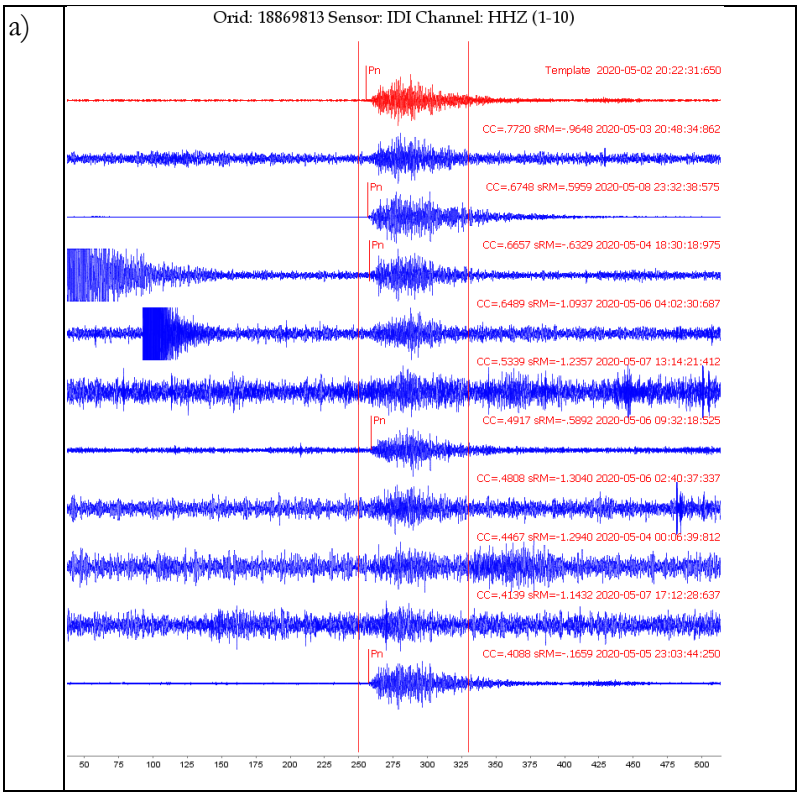

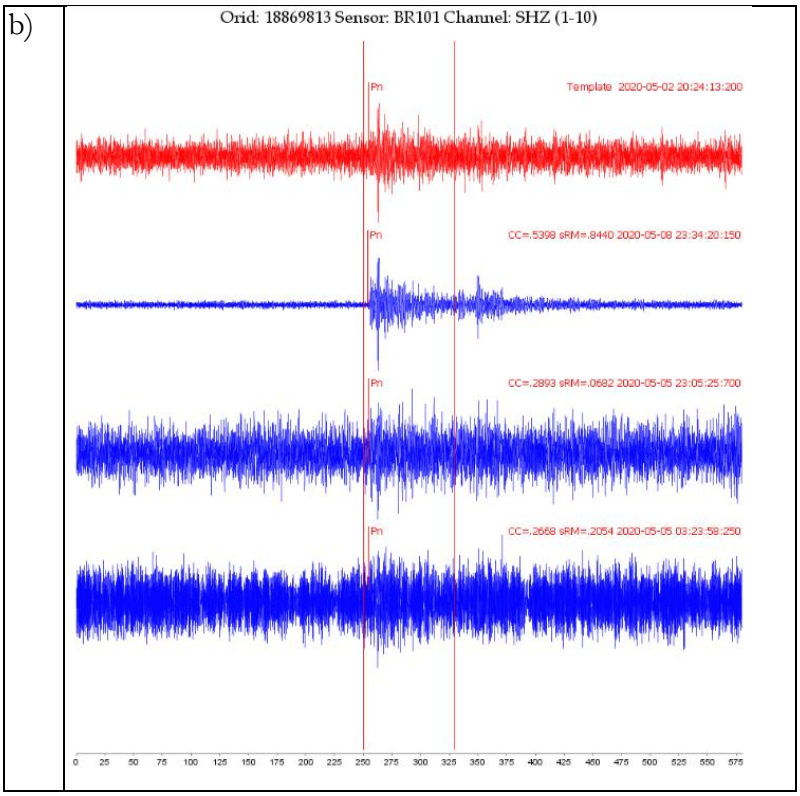

Figure 3-2. Templates (red) based on LEB ORID 18869813 and corresponding correlation detections (blue) to show corroborating detections for repeating events. Template windows are indicated by vertical red lines. a) Pn at IDI. Only the vertical HHZ component is shown for three-component station IDI. b) Pn at BRTR. Only the vertical SHZ of array element BR101 is shown for BRTR.

Table 3-1. Table of relative time calculations for corroborating templates from LEB ORID 18869813 and two sets of correlation detections shown in Figure 3-2.

LEB ORID 18869813						
Detection	Station	Phase	Template date/time (UTC)	Detection date/time (UTC)	Difference in Template Times Relative to IDI (s)	Difference in Detection Times Relative to IDI (s)
1	IDI	Pn	5/2/2020 20:22	5/8/2020 23:32	0	0
1	BRTR	Pn	5/2/2020 20:24	5/8/2020 23:34	102	102
2	IDI	Pn	5/2/2020 20:22	5/5/2020 23:03	0	0
2	BRTR	Pn	5/2/2020 20:24	5/5/2020 23:05	102	101

3.2. 2017 Iran/Iraq Border Aftershocks

We applied waveform correlation to an aftershock sequence that occurred on the border of Iran/Iraq in 2017. There were only 39 candidate template events with associated regional phases for the geographical and temporal extents (Table 2-1), which resulted in small template libraries for each station (Table 2-3, Table 2-4). We processed more stations for the Iran/Iraq border aftershocks to compensate for the small number of templates per station, with the goal of developing enough templates to detect events with multiple stations. The method that was planned for this study only works for template events with associated arrivals from a group of stations. With few templates from each template event, there is little possibility of corroboration by multiple stations. The 2017 Iran/Iraq border aftershock sequence had insufficient template events during the first 24 hours of the aftershock sequence that provided template waveforms for multiple stations. We determined that for this aftershock sequence, the method to apply template event metadata to corroborate arrivals yielded inconclusive results because more data are required. These results are not a failure of the method, but a recognition of the exigencies of the approach and the specific dataset chosen.

We made an adjustment in the study method to provide a workaround for the small template libraries. In prior application of waveform correlation to aftershocks [1][5][6], we used the multistation validation feature of SeisCorr to group waveform correlation detections coincident in time and location into candidate events. The multistation validation algorithm allows detections from any templates, regardless of template event, as long as the travel time from the template event location fits the user-defined tolerances for event hypothesis creation. The flexibility allows waveforms from different stations to vary in alternate ways due to event-to-station travel paths from non-colocated template and detected events. In other words, it is possible for templates from non-colocated but nearby template events to detect the same event.

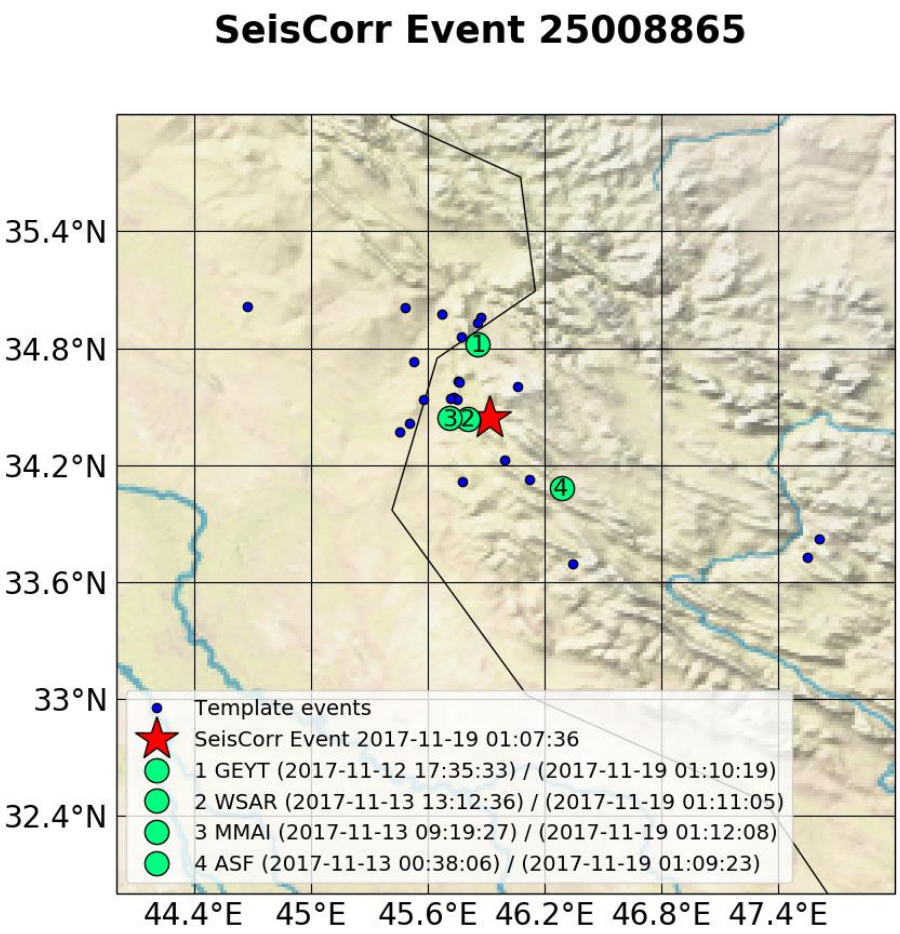

Figure 3-3. Location of SeisCorr event 25008865 detected by waveform correlation, shown by a red star and with the calculated event time in the legend. The four detecting template event locations are shown by green circles with a number corresponding to the detecting station, which is labeled in the legend. The legend shows the template event time followed by the detection time next to each station name. The locations of other template events are indicated by small blue circles.

Figure 3-4 shows an example of the 4-station SeisCorr event 25008865 on a map of the Iran/Iraq border. This example is meant to provide familiarity with the combination of template/detection waveform stacks and a map view of multistation validated events in the figures for the remainder of this section of the report. The location and time of the detected event (red star) were calculated by SeisCorr based on the station detection times, seismic phase of the template, and travel time models. The event was detected by templates from arrays GEYT and MMAI and three-component stations WSAR and ASF. The legend indicates the station name, followed by the template event time and the template detection time.

The template and detected waveforms for SeisCorr event 25008865 are shown for each detecting station in Figure 3-4. The template event times in the legend of Figure 3-4 (e.g., GEYT 2017-11-12 17:35:33) will always precede the template times of Figure 3-4 (e.g., GYA0 2017-11-12 17:38:00) because of the travel time from the event to the station. Templates from four different template events detected the aftershock event within tolerances of 100 km and 50 s. Long template windows were chosen to ensure a high time-bandwidth product; this typically results in detections with more

credibility. For example, the ASF template (Figure 3-4) contains multiple seismic phases in a 260 second-long template with high amplitudes near the 200 sec mark. Templates that incorporate the Lg waveforms are valuable detectors due to high time-bandwidth characteristics of that phase [12][13].

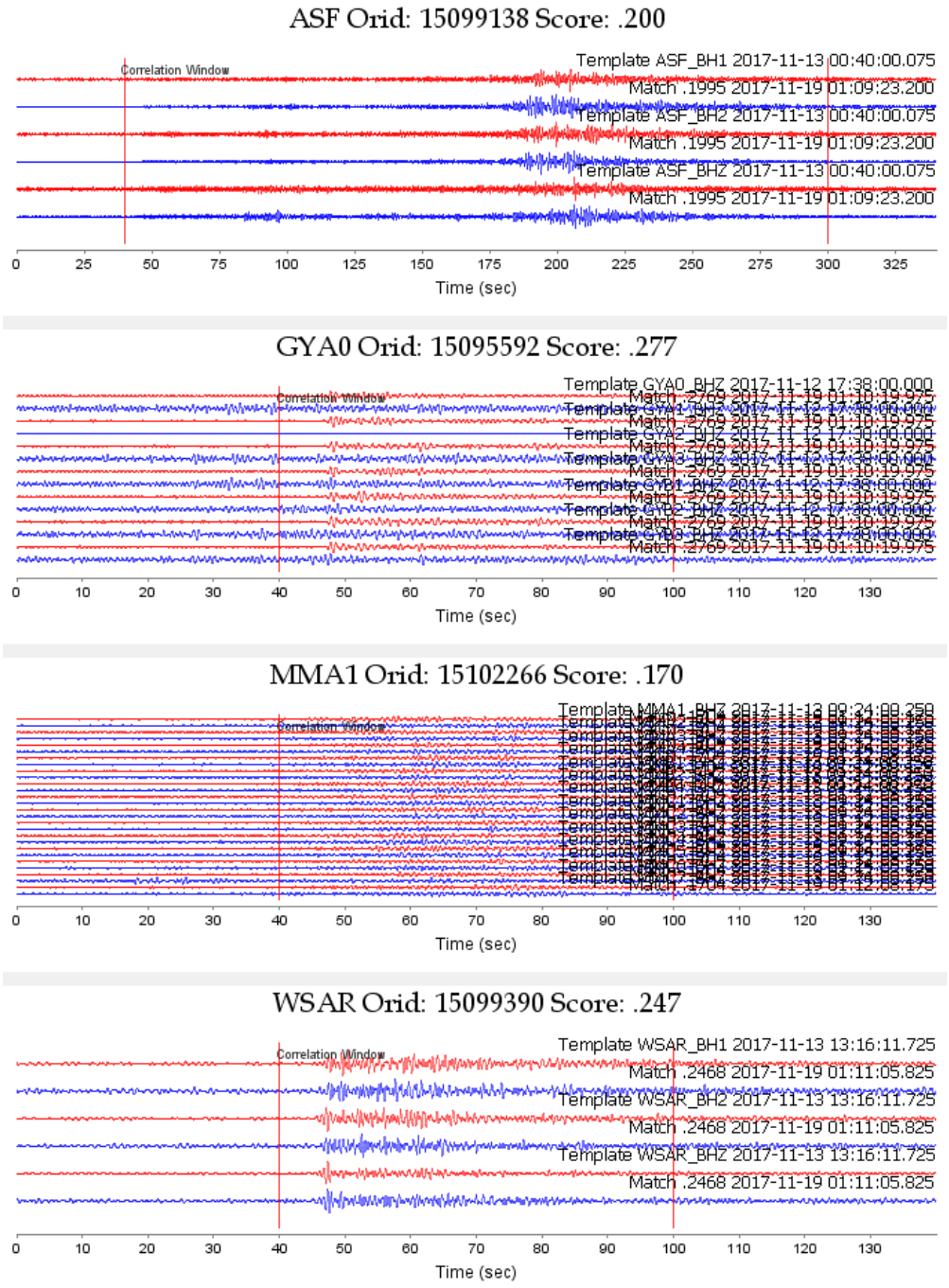

Figure 3-4. Example of 4-station SeisCorr event 25008865 with detections by ASF, GEYT, MMAI and WSAR. The template event ORID and the correlation score are shown above the waveforms. The template waveform is shown in red and the detection waveform is shown in blue, and the channels are shown in red/blue pairs for visual comparison. The template time is 5 s before the picked arrival time. The match time is the same as the detection time shown in the legend of Figure 3-3.

Using multistation validation, we group coincident detections and then analyze them for examples where templates from the same template event detected a later event. An event that has been independently detected by multiple templates from the same template event is typically a more credible detection and thus more worthy of presentation to an analyst reviewing waveform correlation detections. Figure 3-5 shows a set of events detected by waveform correlation that have multiple detections based on the same template event, but from different stations. This figure may motivate future research into the way waveform correlation detections could be presented to seismic analysts to build confidence in events that are detected by multiple stations. The figure is organized to show a different event on each row (e.g., the top row shows SeisCorr event 25008728), and with a pair of waveforms in the left panel and a map of event locations in the right panel.

Event 25008728 was detected by three stations – arrays GEYT and MMAI, and three-component station KBZ. The GEYT and MMAI template waveforms that detected event 25008728 were based on template event 15099741 (Figure 3-5 a). The calculated event time and location are indicated by a red star on the map (Figure 3-5 b). The duplicated detections by template event ORID 15099741 are indicated by the same event time for MMAI and GEYT in the legend, and by the overlapping template event location (green circle) for MMAI (1) and GEYT (3). The calculated event location is closer to the template event location of MMAI and GEYT, as expected.

Event 25008745 was detected by two stations, arrays GEYT and MMAI. The GEYT and MMAI template waveforms that detected event 25008745 were based on template event 15099741 (Figure 3-5 c), which is the same template event that detected events 25008728 (a, b) and 25008885 (i, j). The calculated event location on the map is the same as the template event location, shown as the red star overlaid by the green circles (Figure 3-5 d).

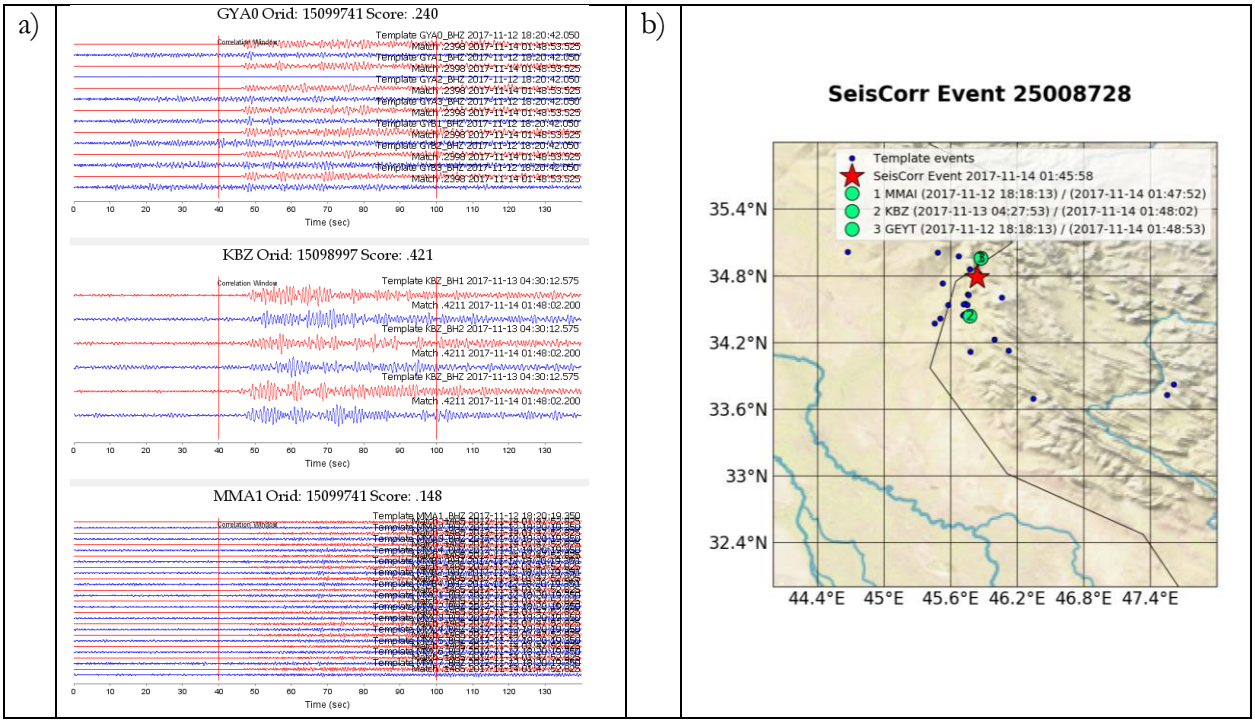

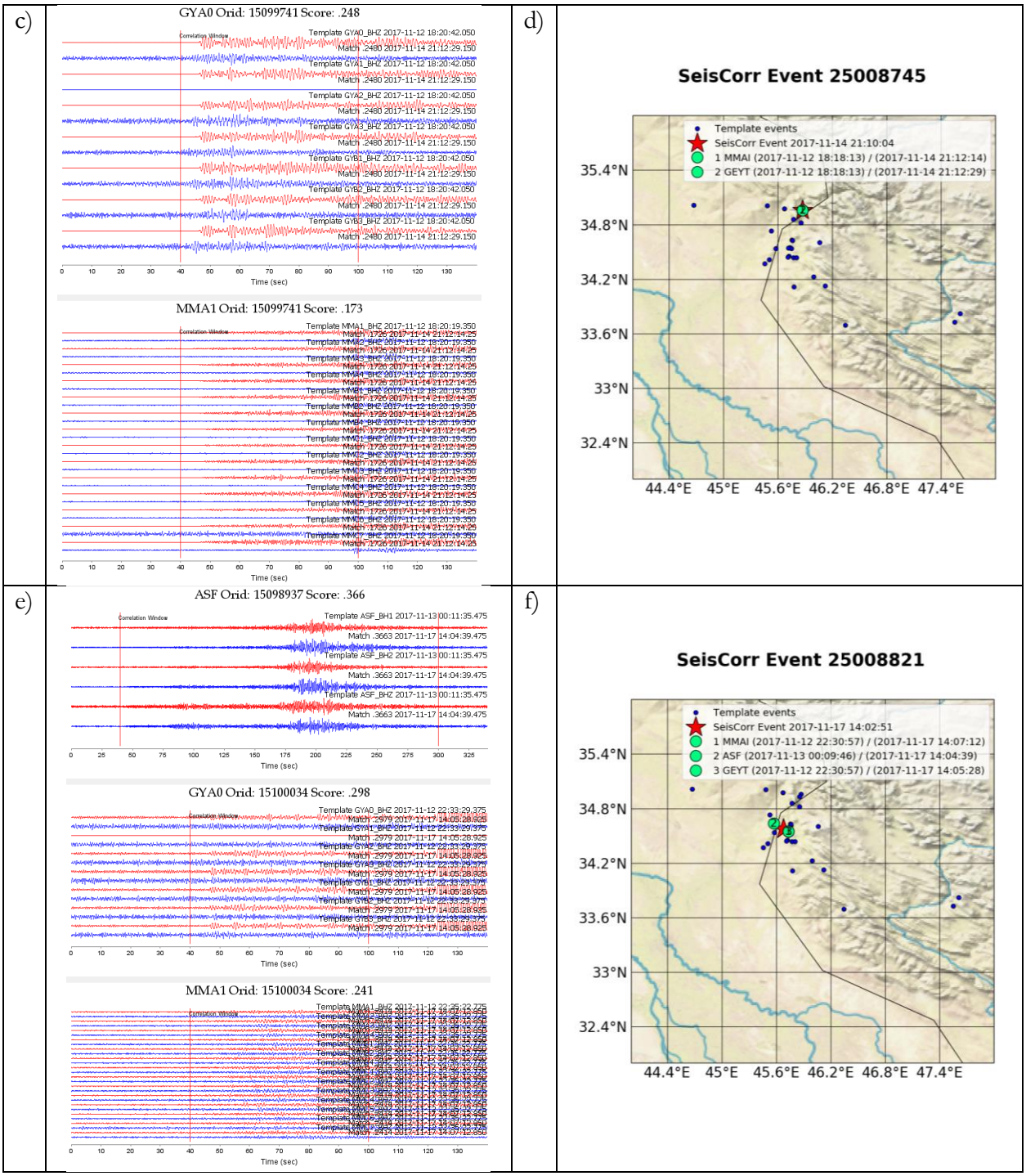
c)
GYA0 Orid: 15099741 Score: .248
Correlation Window
Template GYA0_BHZ 2017-11-12 18:20:42.050
Match .2480 2017-11-14 21:12:29.150
Template GYA1_BHZ 2017-11-12 18:20:42.050
Match .2480 2017-11-14 21:12:29.150
Template GYA2_BHZ 2017-11-12 18:20:42.050
Match .2480 2017-11-14 21:12:29.150
Template GYA3_BHZ 2017-11-12 18:20:42.050
Match .2480 2017-11-14 21:12:29.150
Template GYB1_BHZ 2017-11-12 18:20:42.050
Match .2480 2017-11-14 21:12:29.150
Template GYB2_BHZ 2017-11-12 18:20:42.050
Match .2480 2017-11-14 21:12:29.150
Template GYB3_BHZ 2017-11-12 18:20:42.050
Match .2480 2017-11-14 21:12:29.150
0 10 20 30 40 50 60 70 80 90 100 110 120 130
Time (sec)
MMA1 Orid: 15099741 Score: .173
Correlation Window
Template MMA1_BHZ 2017-11-12 18:20:19.350
Match .1726 2017-11-14 21:12:14.25
Template MMA2_BHZ 2017-11-12 18:20:19.350
Match .1726 2017-11-14 21:12:14.25
Template MMA3_BHZ 2017-11-12 18:20:19.350
Match .1726 2017-11-14 21:12:14.25
Template MMA4_BHZ 2017-11-12 18:20:19.350
Match .1726 2017-11-14 21:12:14.25
Template MME1_BHZ 2017-11-12 18:20:19.350
Match .1726 2017-11-14 21:12:14.25
Template MME2_BHZ 2017-11-12 18:20:19.350
Match .1726 2017-11-14 21:12:14.25
Template MME3_BHZ 2017-11-12 18:20:19.350
Match .1726 2017-11-14 21:12:14.25
Template MME4_BHZ 2017-11-12 18:20:19.350
Match .1726 2017-11-14 21:12:14.25
Template MMV1_BHZ 2017-11-12 18:20:19.350
Match .1726 2017-11-14 21:12:14.25
Template MMV2_BHZ 2017-11-12 18:20:19.350
Match .1726 2017-11-14 21:12:14.25
Template MMV3_BHZ 2017-11-12 18:20:19.350
Match .1726 2017-11-14 21:12:14.25
Template MMV4_BHZ 2017-11-12 18:20:19.350
Match .1726 2017-11-14 21:12:14.25
Template MMV5_BHZ 2017-11-12 18:20:19.350
Match .1726 2017-11-14 21:12:14.25
Template MMV6_BHZ 2017-11-12 18:20:19.350
Match .1726 2017-11-14 21:12:14.25
Template MMV7_BHZ 2017-11-12 18:20:19.350
Match .1726 2017-11-14 21:12:14.25
0 10 20 30 40 50 60 70 80 90 100 110 120 130
Time (sec)
d)
SeisCorr Event 25008745
Template events
SeisCorr Event 2017-11-14 21:10:04
1 MMAI (2017-11-12 18:18:13) / (2017-11-14 21:12:14)
2 GEYT (2017-11-12 18:18:13) / (2017-11-14 21:12:29)
35.4°N
34.8°N
34.2°N
33.6°N
33°N
32.4°N
44.4°E 45°E 45.6°E 46.2°E 46.8°E 47.4°E
e)
ASF Orid: 15098937 Score: .366
Correlation Window
Template ASF_BH1 2017-11-13 00:11:35.475
Match .3663 2017-11-17 14:04:39.475
Template ASF_BH2 2017-11-13 00:11:35.475
Match .3663 2017-11-17 14:04:39.475
Template ASF_BHZ 2017-11-13 00:11:35.475
Match .3663 2017-11-17 14:04:39.475
0 25 50 75 100 125 150 175 200 225 250 275 300 325
Time (sec)
GYA0 Orid: 15100034 Score: .298
Correlation Window
Template GYA0_BHZ 2017-11-12 22:33:29.375
Match .2979 2017-11-17 14:05:28.925
Template GYA1_BHZ 2017-11-12 22:33:29.375
Match .2979 2017-11-17 14:05:28.925
Template GYA2_BHZ 2017-11-12 22:33:29.375
Match .2979 2017-11-17 14:05:28.925
Template GYA3_BHZ 2017-11-12 22:33:29.375
Match .2979 2017-11-17 14:05:28.925
Template GYB1_BHZ 2017-11-12 22:33:29.375
Match .2979 2017-11-17 14:05:28.925
Template GYB2_BHZ 2017-11-12 22:33:29.375
Match .2979 2017-11-17 14:05:28.925
Template GYB3_BHZ 2017-11-12 22:33:29.375
Match .2979 2017-11-17 14:05:28.925
0 10 20 30 40 50 60 70 80 90 100 110 120 130
Time (sec)
MMA1 Orid: 15100034 Score: .241
Correlation Window
Template MMA1_BHZ 2017-11-12 22:33:29.375
Match .2414 2017-11-17 14:07:12.850
0 10 20 30 40 50 60 70 80 90 100 110 120 130
Time (sec)
f)
SeisCorr Event 25008821
Template events
SeisCorr Event 2017-11-17 14:02:51
1 MMAI (2017-11-12 22:30:57) / (2017-11-17 14:07:12)
2 ASF (2017-11-13 00:09:46) / (2017-11-17 14:04:39)
3 GEYT (2017-11-12 22:30:57) / (2017-11-17 14:05:28)
35.4°N
34.8°N
34.2°N
33.6°N
33°N
32.4°N
44.4°E 45°E 45.6°E 46.2°E 46.8°E 47.4°E

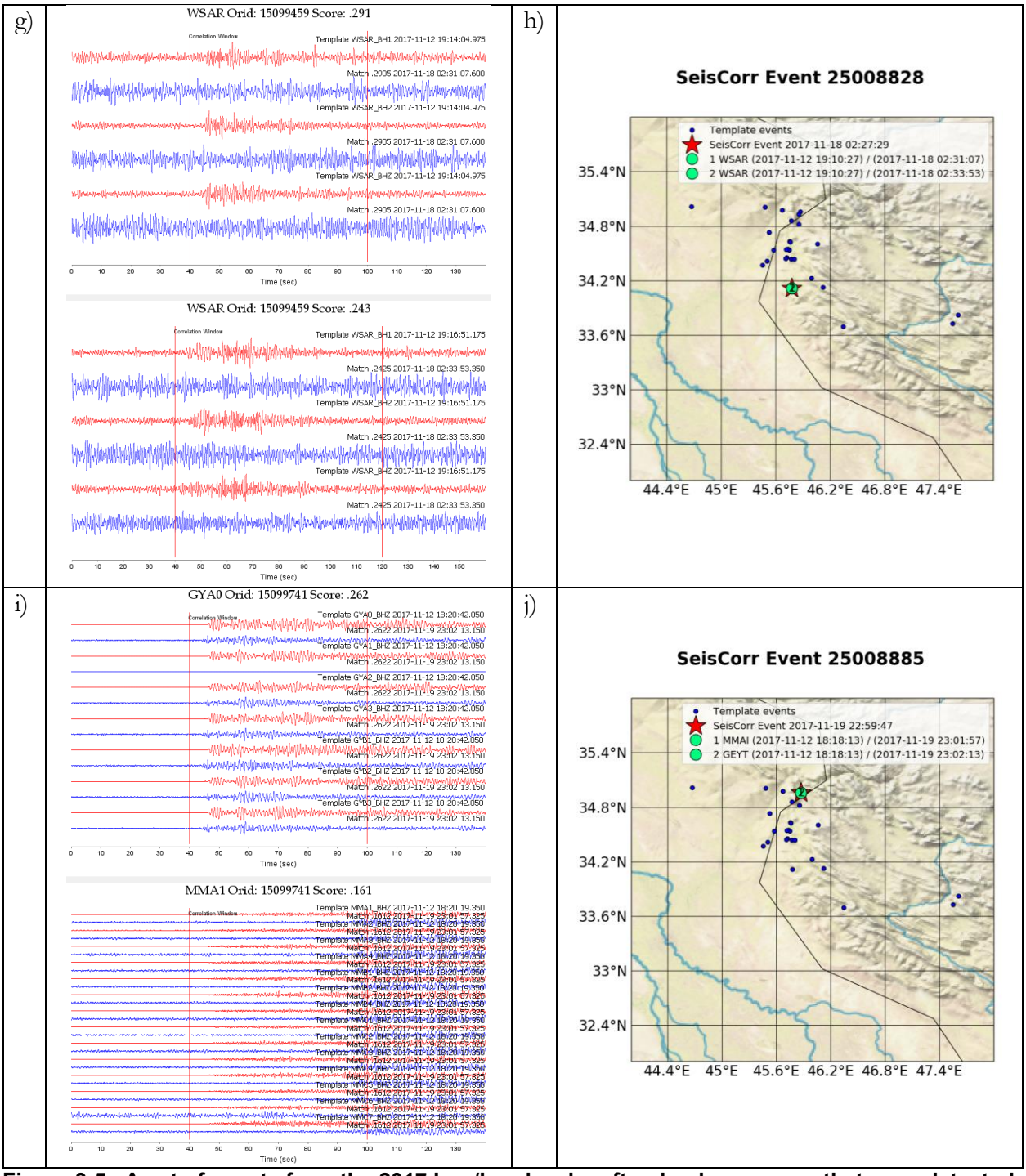

Figure 3-5. A set of events from the 2017 Iran/Iraq border aftershock sequence that were detected by waveform correlation and that have multiple detections based on the same template event and were detected by different stations. The figure is organized to show a different event on each row, and with a pair of waveforms in the left panel (panels a, c, e, g, i) and a map of event locations in the right panel (panels b, d, f, h, j). The rows are organized by increasing event time. The tolerances used were (distance: 100 km, time: 50 s) for the multistation validation event detections shown in the figure. The stations that detected with templates from the same template event can be identified by the template ORID on the left waveform panel (e.g., GEYT and MMAI have detections based on template ORID 15099741 in panel a) and the template event time on the right

map panel (e.g., MMAI and GEYT both show template event times 2017-11-12 18:18:13 in the legend of panel b) and the template circle locations precisely overlap on the map where the template event is located.

Event 25008821 was detected by three stations: arrays GEYT and MMAI and three-component station ASF. The GEYT and MMAI template waveforms that detected event 25008821 were based on template event 15100034 (Figure 3-5 e), but in this case the MMAI template waveform is an Lg pick while the GEYT and ASF template waveforms are Pn picks. ASF has a Pn template based on template event 15100034, but it did not record a detection coincident with the timeframe of 25008821.

Event 25008828 is an interesting example because it was detected by only one station, WSAR, but was detected by templates of two seismic phases, Pn and Sn (Figure 3-5 g). Viewed individually these detections are not convincing because the arrival waveform is buried in noise. Yet the detection by both the Pn and Sn waveforms suggests that there is enough signal present to trigger a match on both phases. The templates do not overlap and so may be considered independent detections.

Similar to event 25008745 (Figure 3-5 c, d), event 25008885 was detected only by two stations, arrays GEYT and MMAI with template waveforms based on template event 15099741 (Figure 3-5 i). With several events in our series based on the same template event, it seems prudent to review the detections for any evidence that the detections may be false. Figure 3-6 shows the template waveforms and detection waveforms for template event 15099741. The three detections shown for GEYT (a) appear to be real events even though the correlation scores are low and range from 0.2622 to 0.2398; the template threshold calculated by the time-reverse method is 0.23. In contrast, the set of low correlation score matches for MMAI (b) contains a mix of detections that appear legitimate and detections that are questionable. Waveforms are ordered by correlation score from top to bottom and range from 0.1793 to 0.1421 with a template threshold of 0.14. Event 25008728 is based on a detection with a waveform that appears similar to the template waveform, although smaller in amplitude. Based on correlated signals from other stations, we know that events 25008745 and 25008885 are real events, but the correlation detections do not seem to correspond to the template (shown at the top), and instead seem to be false correlations with unrelated signals that that begin at the end of the template window and extend to the right. Clearly, matches that are based on a small portion of the template window are a problem, as we have seen in prior correlation studies. From this review we can see that several MMAI detections are wrongly correlated with this template waveform even though the events they corroborate are real.

This example (Figure 3-6) shows that requiring multiple detections by template waveforms be based on the same template event does not preclude faulty correlation detections, particularly when working with low template detection thresholds. Moreover, as we saw with station MMAI, it is interesting that the wrongly correlated waveforms can have a higher correlation score than the likely correctly correlated waveforms. These unintuitive correlation scores may be due to the unrealistic matched filter null hypothesis that a waveform will contain either a scaled copy of the waveform that is being matched, or gaussian noise, but no seismic waveforms from other sources [8][9]. Figure 3-6 b shows a clear example where simply raising the correlation threshold will exclude correct detections as well as incorrect detections and motivates the need for additional research to improve on techniques used for seismic waveform pattern matching [8][9][10]. One possible avenue is machine learning, where initial investigations using a paired neural network and constructed

waveforms have shown promise in addressing the shortfalls of waveform correlation as applied to aftershock sequences [14].

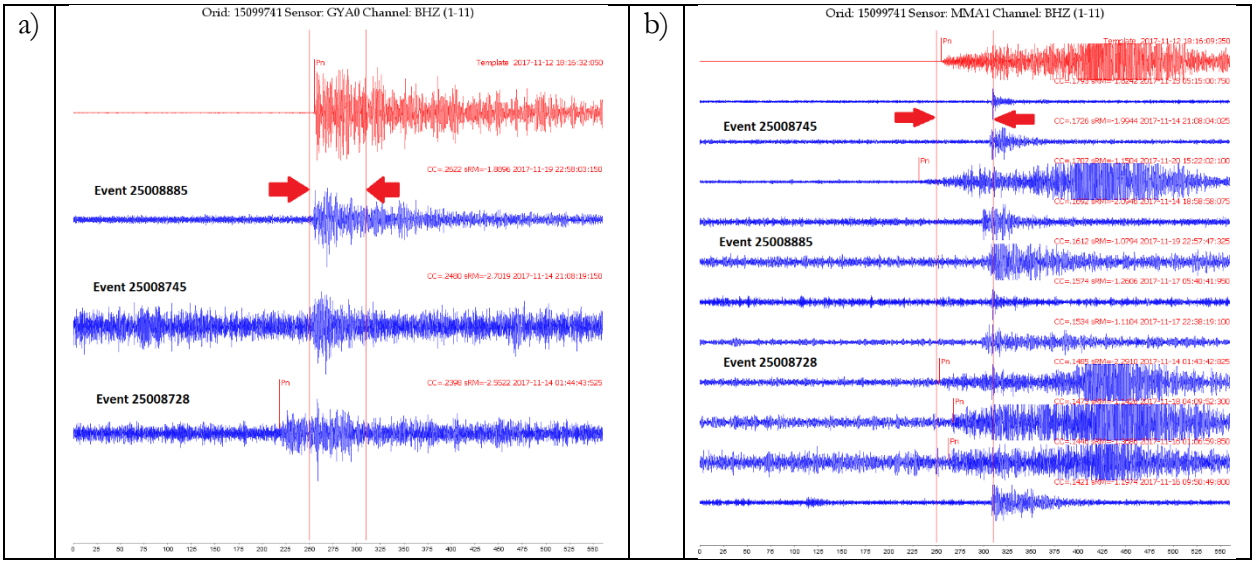

Figure 3-6. Template waveforms (red) and detection waveforms (blue) for template event 15099741 for GEYT (a) and MMAI (b). The event numbers corresponding to the waveforms in Figure 3-5 are superimposed on the figure. The red arrows indicate the width of the template window for calculating the correlation score and determining whether there is a match above the template threshold.

4. DISCUSSION

Waveform correlation is an established technique for finding repeating events. However, using waveform correlation only as a signal detector does not guarantee a reduction in analyst workload if marginal events that do not meet bulletin-inclusion criteria are detected and passed on to the analyst for review. Our research targets the selection of waveform correlation detections that will lead to bulletin-worthy events. Traditional waveform correlation works extremely well for dense networks and local distances where the template has a high time-bandwidth product for a high SNR waveform. This study seeks to stretch the application of the technique to sparse global networks by using additional information beyond the waveform to develop supporting evidence for a credible repeating event. A combined group of corroborating arrivals at other stations consistent in time with a repeating event and a simple calculation of relative times can establish the credibility of the repeating event and lead to a relative location.

In a prior study of mining blast events [4] we used template event metadata to create a set of corroborating templates, some of which were so marginal that they would not pass SNR threshold tests or STA/LTA threshold tests. Yet, a group of marginal mining blast detections based on the same template event was convincing when relative times were analyzed between the templates and detections for multiple stations. In that study, we proposed a set of criteria (based on metadata from the template event and the detection) that select waveform correlation detections of mining blast events that are most likely to result in bulletin-worthy events.

The goal of this study was to apply the same method to a different type of repeating event, aftershocks, and in a different region, the Middle East. We chose two aftershock sequences in the Middle East, one on May 2, 2020 southeast of Crete and one on November 13, 2017 on the Iran/Iraq border. We created waveform templates based on the first 24 hours of the aftershock sequence for stations at local to regional distances, then correlated the templates with continuous waveform data for the next week. Results were analyzed for evidence that template event metadata may be used to improve the selection of waveform correlation detections such that only the detections most useful to the analysts can be identified. Moreover, we sought cases showing that template event metadata can lead to additional templates and detections that augment the evidence for a repeating event hypothesis by calculating relative times for the template and detection based on the initial waveform correlation time.

The study results were mixed. In the case of the 2020 Crete aftershock sequence, there were examples of waveform correlation detections that could be expanded through use of template event metadata to develop additional evidence for a repeating event hypothesis; in other words, the method worked as expected. However, the examples were less numerous than anticipated and the study was disadvantaged by stations with data recording errors during critical timeframes. The 2017 Iran/Iraq border aftershock sequence was even more challenging, because there were only 39 candidate template events from which to make template waveforms, which led us to seek an alternate approach using our previously established multistation validation method to identify template events that could lead to detections by multiple stations. The results for this aftershock sequence were disadvantaged because there were not enough template events to successfully apply the method.

Our results suggest that the method offers potential benefits, but the choice of aftershock sequences, stations, and template parameters led to inconclusive but encouraging results. Our recommendation for future research is to continue to investigate the method to improve waveform correlation detections for aftershock sequences along similar lines of inquiry, but with additional

datasets. The method could be explored with modifications to the study, such as application to regions with denser station coverage, shorter template windows to reduce event overlaps, a longer time period for candidate templates and aftershock detections (e.g., a week of templates and a month of detections), and the choice of alternate regions and aftershock sequences with fewer data recording issues and denser template event coverage. Additionally, we observed examples that suggest waveform pattern matching and threshold setting may be particularly challenged in the presence of aftershock events and recommend further study of the impact of matched filter hypothesis assumptions for aftershock identification.

If our proposed method is proven successful, there is a significant benefit that could be realized by the method of using template event metadata to develop corroborating arrivals. Only template waveforms from stations at local or regional distances need to be curated as template libraries for the initial waveform correlation detection because the corroborating templates can theoretically be windowed on demand based on metadata of recorded arrival times in the template event. We acknowledge that more complexity is needed to dynamically window waveforms and set thresholds for the corroborating arrivals, but once the system is developed it may be particularly useful for aftershock sequences that can occur in any seismically active zone.

In conclusion, aftershocks are a frequent source of seismic events that must be dealt with on a global scale by monitoring agencies. Waveform correlation is well-suited to detecting such events because of their similar waveform characteristics due to geographically colocated sources. Using template event metadata to corroborate repeating events is a relatively simple enhancement to traditional waveform correlation that may lead to improved aftershock identification, seismic arrival association and location, and reducing analyst workload during high event rates. More research is needed to determine if our method is suitable to aftershock events. In addition to reducing analyst workload and improving bulletin quality, the potential benefits include improving global monitoring pipeline efficiency by correctly associating groups of aftershock arrivals and reducing the possibility of misassociating aftershocks with other seismic signals.

REFERENCES

[1] Sundermier, A., R. Tibi, and C. J. Young (2019). Applying Waveform Correlation to Aftershock Sequences Using a Global Sparse Network, *Technical Report SAND2019-10184*.

[2] Sundermier, A., R. Tibi, and C. J. Young (2020). Applying Waveform Correlation to Mining Blasts Using a Global Sparse Network*, Technical Report SAND2020-7660*.

[3] Sundermier, A., R. Tibi, R. A. Brogan, and C. J. Young (2021). Applying Waveform Correlation to Reduce Seismic Analyst Workload Due to Repeating Mining Blasts, *Bull. Seismol. Soc. Am.* doi: 10.1785/0120210124.

[4] Sundermier, A., R. Tibi, and C. J. Young. Applying Waveform Correlation and Waveform Template Metadata to Mining Blasts to Reduce Analyst Workload*, Technical Report in preparation for publication.*

[5] Slinkard, M., S. Heck, D. Schaff, N. Bonal, D. Daily, C. Young, and P. Richards (2016). Detection of the Wenchuan Aftershock Sequence Using Waveform Correlation with a Composite Regional Network, *Bull. Seismol. Soc. Am.* **106**, 1371-1379. doi: 10.1785/0120150333.

[6] Slinkard, M. E., D. B. Carr, and C. J. Young (2013). Applying waveform correlation to three aftershock sequences, *Bull. Seismol. Soc. Am.* **103**, 675-693. doi: 10.1785/0120120058.

[7] Slinkard, M., D. Schaff, N. Mikhailova, S. Heck, C. Young, and P. G. Richards (2014). Multistation validation of waveform correlation techniques as applied to broad regional monitoring, *Bull. Seismol. Soc. Am.* **104**, 2768-2781. doi: 10.1785/0120140140.

[8] Carmichael, J. D. and H. Hartse (2016). Threshold Magnitudes for a Multichannel Correlation Detector in Background Seismicity, *Bull. Seismol. Soc. Am.* **106**, 478–498. doi: 10.1785/0120150191.

[9] Ganter, T., A. Sundermier, and S. Ballard (2018). Alternate Null Hypothesis Correlation: A New Approach to Automatic Seismic Event Detection, *Bull. Seismol. Soc. Am.* **108**, 3528-3547. doi: 10.1785/0120180074.

[10] Tibi, R., C. Young, A. Gonzales, S. Ballard, and A. Encarnacao (2017). Rapid and robust cross-correlation-based seismic signal identification using an approximate nearest neighbor method, *Bull. Seismol. Soc. Am.* **107**, 1954–1968. doi: 10.1785/0120170011.

[11] Tibi, R., P. Hammond, R. Brogan, C. J. Young, and K. Koper (2021). Deep Learning Denoising Applied to Regional Distance Seismic Data in Utah, *Bull. Seismol. Soc. Am.* **111**, 775-790. doi: 10.1785/0120200292.

[12] Schaff, D. P., and P. G. Richards (2004). Lg-wave cross correlation and double difference location: application to the 1999 Xiuyan, China, sequence, *Bull. Seismol. Soc. Am.* **94**, 867-879. doi: 10.1785/0120030136.

[13] Schaff, D. P., P. G. Richards, M. Slinkard, S. Heck, and C. Young (2018). Lg-Wave Cross Correlation and Epicentral Double-Difference Location in and near China, *Bull. Seismol. Soc. Am.* **108**, 1326-1345. doi: 10.1785/0120170137.

[14] Conley, A., B. Donohoe, and B. Greene. Using a Paired Neural Network for Aftershock Identification: Application to Constructed Data, *In preparation for publication.*

DISTRIBUTION

Email—Internal

Name	Org.	Sandia Email Address
Technical Library	01177	libref@sandia.gov

This page left blank

This page left blank

Sandia National Laboratories

Sandia National Laboratories is a multimission laboratory managed and operated by National Technology & Engineering Solutions of Sandia LLC, a wholly owned subsidiary of Honeywell International Inc. for the U.S. Department of Energy's National Nuclear Security Administration under contract DE-NA0003525.